AGU PUBLICATIONS

Paleoceanography

RESEARCH ARTICLE
10.1002/2016PA003057

**Key Points:**
- Uncertainty analysis is based on Monte Carlo realizations of the time series
- Age uncertainties are the main contributor to the overall uncertainty
- Phase relationship needs to be established on a large number of records

**Supporting Information:**
- Supporting Information S1

**Correspondence to:**
D. Khider,
khider@usc.edu

**Citation:**
Khider, D., Ahn, S., Lisiecki, L. E., Lawrence, C. E., & Kienast, M. (2017). The role of uncertainty in estimating lead/lag relationships in marine sedimentary archives: A case study from the tropical Pacific. *Paleoceanography*, *32*. https://doi.org/10.1002/2016PA003057

Received 16 NOV 2016
Accepted 21 OCT 2017
Accepted article online 26 OCT 2017



# The Role of Uncertainty in Estimating Lead/Lag Relationships in Marine Sedimentary Archives: A Case Study From the Tropical Pacific

**D. Khider[1,2], S. Ahn[3], L. E. Lisiecki[2], C. E. Lawrence[3], and M. Kienast[4]**

[1]Department of Earth Science, University of Southern California, Los Angeles, CA, USA, [2]Department of Earth Science, University of California, Santa Barbara, CA, USA, [3]Division of Applied Mathematics, Brown University, Providence, RI, USA, [4]Department of Oceanography, Dalhousie University, Halifax, Nova Scotia, Canada

**Abstract** Understanding the mechanisms behind any changes in the climate system often requires establishing the timing of events imprinted on the geological record. However, these proxy records are prone to large uncertainties, which may preclude meaningful conclusions about the relative timing of events. In this study, we put forth a framework to estimate the uncertainty in phase relationships inferred from marine sedimentary records. The novelty of our method lies in the accounting of the various sources of uncertainty inherent to paleoclimate reconstruction and timing analysis. Specifically, we use a Monte Carlo process allowing sampling of possible realizations of the time series as functions of uncertainties in time, the climate proxy, and the identification of the termination timing. We then apply this technique to 15 published sea surface temperature records from the equatorial Pacific to evaluate whether we observed any significant changes in the termination timing between the east and the west. We find that the uncertainty on the relative timing estimates is on the order of several thousand years and mainly stems from age model uncertainty (90%). However, even small differences in mean termination timings can be detected with a sufficiently large number of samples. Improvements in the dating of sediment records provide an opportunity to reduce uncertainty in studies of this kind.

## 1. Introduction

The most striking features of the climate of the late Quaternary are the repeated changes between glacial and interglacial periods. However, the mechanisms behind these large reorganizations of the climate system are sill poorly understood (Paillard, 2015, for a review and references therein). Two main theories have been put forward to explain these cycles: (1) the astronomical (Milankovitch) hypothesis and (2) a geochemical hypothesis, which highlights the active role of atmospheric $CO_2$ (Paillard, 2015). A central question of climate science has been to quantify the respective roles of the insolation forcing and of greenhouse gases changes (Paillard, 2015). Settling this question will require a better understanding of the physical mechanisms leading to the terminations as well as a better handle on the phase relationship with estimates of the lead or the lag between various components of the climate system (Billups, 2015; Denton et al., 2010; Saikku et al., 2009; Stott et al., 2007; Waelbroeck et al., 2001). Proxy reconstructions can help distinguish among different proposed mechanisms and test paleoclimate models; however, a proper accounting of the uncertainty associated with these records is crucial to assess the significance of any observed differences.

Paleoclimate studies present a unique challenge in the estimation of uncertainty since both errors in the age and the reconstructed parameter need to be accounted for. Traditionally, these errors have been reported separately, a process which may overestimate/underestimate the actual errors associated with the reconstruction since it does not take into account the time sampling of the data. Furthermore, the assumption that the uncertainties can be described as random and independent is often not justified. For instance, the interpolation scheme in between age control time points is a source of dependent uncertainties. In other words, stratigraphic constraints need to be preserved in the estimation of uncertainty. To this end, a variety of techniques based on Monte Carlo simulations and Bayesian statistics have been developed and used by the ice core community (e.g., Mudelsee, 2000; Parrenin et al., 2013; Röthlisberger et al., 2008; Schmitt et al., 2012), in sea level studies (e.g., Grant et al., 2012; Kopp et al., 2009; Rohling et al., 2014; Sambridge, 2016; Stanford et al., 2011), in reconstructions of past climate variability (e.g., Hoffman et al., 2017; Khider et al., 2015, 2014;

Marcott et al., 2013; Marino et al., 2015; Shakun et al., 2012; Tierney & Tingley, 2014; Thirumalai et al., 2016), and in age modeling (e.g., Blaauw & Christen, 2011; Breitenbach et al., 2012; Comboul et al., 2014; Haslett & Parnell, 2008). Here we present an example of how such techniques can be applied to the analysis of proxy data from marine sediment cores. Marine sediments can provide long and continuous archives of ocean conditions; however, they present further challenges in the estimation of uncertainty since multiple processes can affect the signal in both age and the reconstructed parameter. These include sedimentation rate changes, bioturbation, and sediment distortion due to coring. Therefore, it is important to use methodologies specifically designed for marine sedimentary archives when estimating the uncertainty in these records.

### 1.1. Glacial Terminations

The current preferred paradigm to explain glacial terminations involves the collapse of the Northern Hemisphere ice sheets in response to summer insolation and its effect on the Atlantic Meridional Overturning Circulation (AMOC) (Denton et al., 2010). However, this hypothesis has been called into question by paleorecords, which suggest that tropical sea surface temperatures (SST) led continental ice volume changes (e.g., Lea et al., 2006; Visser et al., 2003). The role of surface ocean conditions in the tropical Pacific in influencing the global climate on interannual and decadal timescales further prompted the hypothesis that the tropical Pacific could play an active role in controlling climate on longer timescales (Broecker & Clark, 2003; Cane, 1998; Clement & Cane, 1999a; 1999b; Pierrehumbert, 2000; Seager & Battisti, 2007), perhaps through hydrological changes and their impacts on the energy budget (Clement & Peterson, 2008), through changes in the mass balance of the Northern Hemisphere ice sheets (Rodgers et al., 2003; Yin & Battisti, 2001), or by exerting a direct control on the thermohaline circulation (Latif et al., 2000; Schmittner & Clement, 2002; Schmittner et al., 2000).

Distinguishing between these competing hypotheses requires an analysis of the timing of SST changes during glacial terminations (Billups, 2015) between the North Atlantic and the tropical Pacific as well as within the tropical Pacific itself. Many modern climate changes around the globe have been forced from the tropical Pacific through various SST and convection patterns (Seager & Battisti, 2007). Because the dominant pattern of interannual tropical climate variability is the El Niño–Southern Oscillation (ENSO), this particular SST pattern has often been invoked to explain the paleorecord on millennial and longer timescales (e.g., Conroy et al., 2010; Koutavas & Lynch-Stieglitz, 2003; Koutavas et al., 2002; Mann et al., 2009; Stott et al., 2002). Although there is modeling evidence (e.g., An et al., 2004; Clement & Cane, 1999a; Otto-Bliesner et al., 2003; Zhang et al., 2008) for orbital changes in ENSO behavior, the spatial pattern of abrupt climate change does not follow the ENSO blueprint, suggesting that an ENSO-like mean state of the tropical Pacific cannot adequately provide a mechanism through which the tropics can affect a global climate response at the glacial terminations (Seager & Battisti, 2007). However, changes in the distribution and strength of tropical convection are capable of affecting midlatitude wind regimes, propagating the deglaciation signal throughout the globe (Lee & Kim, 2003; Son & Lee, 2005). These mechanisms would leave distinct SST patterns across the tropical Pacific, with differences in the timing of SST changes in the eastern (EP) compared to the western Pacific (WP). For instance, an El Niño-like signature (e.g., Koutavas et al., 2002) would manifest as a rise in SST in the EP before the WP while changes in tropical convection (Lee & Kim, 2003) do not require a differential warming within the tropical Pacific.

Furthermore, although recent work has focused on the last glacial termination when independent, radiocarbon-based chronologies can be developed (e.g., Koutavas et al., 2002; Stott et al., 2007; Timmermann et al., 2014), any conclusions about a tropical role in orbital climate change should hold for other terminations as well. Because absolute dating using radiocarbon dating techniques is limited to the last ~40 kyr, relative age models produced by stratigraphic alignments are one of the most common age modeling techniques applied beyond this time frame (Govin et al., 2015; Lang & Wolff, 2011; Shackleton, 1967). This is particularly true for marine sedimentary records. The question then becomes the following: Are these proxy reconstructions precise enough to establish phase relationships among various components of the climate system in order to shed more light on possible mechanisms leading to the glacial terminations?

Here we seek to evaluate whether relative age dating can be used to assess phase relationships among various components of the climate system by testing the tropical Pacific hypothesis using a conceptual framework for the determination of phase relationships, and most importantly their significance, among time-uncertain proxy SST records. This framework allows sampling renditions of the time series based on the uncertainty in age (Lin et al., 2014) and the temperature proxy (Khider et al., 2014). Although the use of Monte Carlo sampling

is not a new concept in the estimation of uncertainty in paleoceanographic reconstructions, a probabilistic alignment algorithm was not available until recently. Furthermore, we quantify the relative contributions of the various sources of uncertainty, which can be used to identify ways to improve future estimates of phase relationships.

## 2. Methods

### 2.1. Data

The timing of glacial terminations across the tropical Pacific (defined here as the latitudinal band from 30°S to 30°N) was assessed from 15 published SST records (Table 1). The SST records were selected based on four criteria: (1) SSTs were derived from either Mg/Ca of the planktonic foraminifer *Globigerinoides ruber* or the $U^{k'}_{37}$ proxy, (2) the resolution of the records was at least 2.5 kyr on average, (3) the records were at least 100 kyr long, and (4) a benthic $\delta^{18}$O record was available for age modeling purposes (section 2.2.1). The 15 data sets are distributed equally between the EP and WP. Our database includes 5 Mg/Ca and 10 $U^{k'}_{37}$ records, allowing an assessment of proxy biases on the timing of the glacial terminations. Since the age model for the MD05-2920 record (WP, Table 1; Tachikawa et al., 2014) could be derived from two benthic curves based on *Uvigerina peregrina* and *Cibicidoides wuellerstorfi*, respectively, we treated the SST time series as two distinct records. Here we used the SST time series obtained from the alignment based on *U. peregrina* as the reference to infer the relative termination timing across the tropical Pacific. Because both time series have a similar temporal resolution (0.15 kyr) and similar number of data points ($n = 242$ for the series based on *Uvigerina peregrina* and $n = 234$ for the series based on *Cibicidoides wuellerstorfi*), choosing one record over the other as the reference should not affect the analysis. Comparing the relative termination timing between the two alignments for MD05-2920 further allows testing the sensitivity of our technique to the various sources of uncertainty, which are detailed in the following section.

### 2.2. Uncertainty Quantification

The uncertainty associated with the timing of the glacial terminations includes the uncertainty in the age model, the uncertainty in the SST reconstruction, and the uncertainty in timing of SST changes, which we assessed based on change points. To take into account these various sources of uncertainty in our estimates of the relative timing of the glacial terminations in the EP and the WP, we used a Monte Carlo approach ($n = 1{,}000$ trials), in which we created possible realizations of the time series (Khider et al., 2014), which are a function of the uncertainties in the benthic $\delta^{18}$O alignment in abscissa and analytical and calibration errors in ordinates. The timing of glacial terminations, that is, the change point, was then assessed on each Monte Carlo realization of the time series. A review of each of these sources of uncertainty and their treatment in the Monte Carlo scheme is described below and illustrated in Figure 1.

#### 2.2.1. Age Model

The age model for each of the records considered in this study was based on the alignment to the global benthic $\delta^{18}$O stack of Lisiecki and Raymo (2005, hereafter LR04) using a Hidden Markov model probabilistic alignment algorithm (HMM-Match) (Lin et al., 2014). The advantage of this algorithm over the more traditional manual, qualitative comparison (Prell et al., 1986; Shackleton et al., 2000) or deterministic algorithms (e.g., Huybers & Wunsch, 2004; Lisiecki & Lisiecki, 2002; Martinson et al., 1987) is its ability to sample directly and exactly from the distribution of ages given the data and to use these samples to construct 95% confidence bands for the alignment by considering the probability of every possible alignment based on its fit to the $\delta^{18}$O data (the emission model, which is based on benthic $\delta^{18}$O residuals) and transition probabilities for sedimentation rate changes (Lin et al., 2014). Since the emission model and transition probabilities are modeled for marine sediment cores, alignment to ice core or speleothem chronologies is not possible at this time. Here we considered each of the 1,000 alignments returned by the algorithm as a possible age model for the Monte Carlo time series. The benthic $\delta^{18}$O alignments for each of the records considered in this study along with their estimated uncertainties are presented in the supporting information.

The HMM-Match uncertainty does not include the absolute uncertainty in the age of the LR04 stack, which does not need to be considered for the determination of the relative timing. However, relative age modeling requires the assumption that the deglacial onset of benthic $\delta^{18}$O changes are globally synchronous and can, therefore, directly be derived from the LR04 global stack. A review of seven regional benthic $\delta^{18}$O stacks with independent radiocarbon age models suggests that the termination onset occurred ~1 kyr later in the intermediate Pacific (1000–2000 m water depth) than in the deep Pacific (Stern & Lisiecki, 2014). Since the records

**Table 1**
*SST Records Considered in This Study*

| Name | Lon °E | Lat °N | Water depth (m) | Period (kyr) | Res (kyr) | Age CI (kyr) | Proxy | Reference |
|---|---|---|---|---|---|---|---|---|
| LPAZ-21P | −109.5 | 23.0 | 624 | 1–236 | 1.3 | 8.7 | $U^{k'}_{37}$ | Herbert et al. (2001) |
| MD05-2920 | 144.5 | −2.9 | 1,843 | 0–388 | 0.7 | 5.0 | Mg/Ca | Tachikawa et al. (2014) |
| MD06-3067 | 126.5 | 6.5 | 1,575 | 4–158 | 0.4 | 1.6 | Mg/Ca | Bolliet et al. (2011) |
| ODP1143 | 113.3 | 9.4 | 2,272 | 0–403 | 1.7 | 9.2 | $U^{k'}_{37}$ | Cheng et al. (2004); Li et al. (2011) |
| ODP1146 | 116.2 | 19.5 | 2,091 | 5–400 | 2 | 4.5 | $U^{k'}_{37}$ | Herbert et al. (2010) |
| ODP1012 | −118.4 | 32.3 | 1,783 | 2–400 | 1.2 | 5.1 | $U^{k'}_{37}$ | Brierley et al. (2009) |
| ODP1145 | 117.6 | 19.6 | 3,175 | 2–143 | 0.5 | 4.1 | Mg/Ca | Oppo and Sun (2007) |
| ODP846 | −90.8 | −3.1 | 3,296 | 4–400 | 2.5 | 6.3 | $U^{k'}_{37}$ | Lawrence et al. (2006) |
| TR163-19 | −91.0 | 2.3 | 2,348 | 0–361 | 1.7 | 5.9 | Mg/Ca | Lea et al. (2002, 2006) |
| TR163-19 | −91.0 | 2.3 | 2,348 | 0–36 | 1.7 | 5.9 | $U^{k'}_{37}$ | Dubois et al. (2009) |
| TR163-22 | −92.4 | 0.5 | 2,830 | 1–135 | 0.3 | 2.1 | Mg/Ca | Lea et al. (2006) |
| MJ0005A-27JC | −82.8 | −1.9 | 2,203 | 3–163 | 0.8 | 3.4 | $U^{k'}_{37}$ | Dubois et al. (2009) |
| MD97-2151 | 109.9 | 8.7 | 1,598 | 1–145 | 0.1 | 2.1 | $U^{k'}_{37}$ | Zhao et al. (2006) |
| MD06-3075 | 125.9 | 6.5 | 1,878 | 0–115 | 0.4 | 2.5 | $U^{k'}_{37}$ | Fraser et al. (2014) |
| ODP1239 | −82.1 | −0.7 | 1,414 | 0–500 | 1.6 | 6.1 | $U^{k'}_{37}$ | Rincón-Martínez et al. (2010) |

*Note.* We use the MD05-2920 record with the age model based on *U. peregrina* as reference to calculate the relative timing of the terminations. For long records, only the first 300 kyr of record was used and aligned for computation speed. Lon: Longitude, Lat: Latitude, Res: Resolution, CI: 95% confidence interval width.

considered in this study include cores extending across this boundary, we will also evaluate the relative timing of SST changes based on the intermediate and deep sites, respectively (section 3.2.2).

### 2.2.2. Sea Surface Temperature

SSTs for the records used in this study were derived from either the *G. ruber* Mg/Ca or the $U^{k'}_{37}$ proxy. We considered two sources of uncertainty in the SST estimates: the analytical uncertainty on the Mg/Ca or $U^{k'}_{37}$ measurements, which we assumed to be normally distributed and independent from sample to sample, and the uncertainty in the calibration equation, which would affect a group of measurements similarly (i.e., only one equation is used to obtain SSTs for each downcore record). We combined these sources of uncertainty in the Monte Carlo simulations using Bayesian inference, which allowed us to enumerate possible solutions for the calibration equation (Khider et al., 2015). Bayesian statistics is a framework permitting inferences on the uncertain parameters (in this case, the coefficients of the calibration equation), which can be updated as new information (data) becomes available. Bayes' rule takes the form

$$\pi(\text{unknowns} \mid \text{data}) \propto f(\text{data} \mid \text{unknowns}) \cdot \pi(\text{unknowns})$$

The term $\pi(\text{unknowns} \mid \text{data})$ represents the probability of the unknown given the data and is called the posterior distribution; $f(\text{data} \mid \text{unknowns})$ is the likelihood of the data given the unknowns; and $\pi(\text{unknowns})$ is the prior information of the unknowns, which encode previous information about the unknowns available before the current data have been analyzed. For the Mg/Ca and $U^{k'}_{37}$ calibration models considered here, the unknowns represent the regression coefficients. Following the original studies referenced in Table 1,

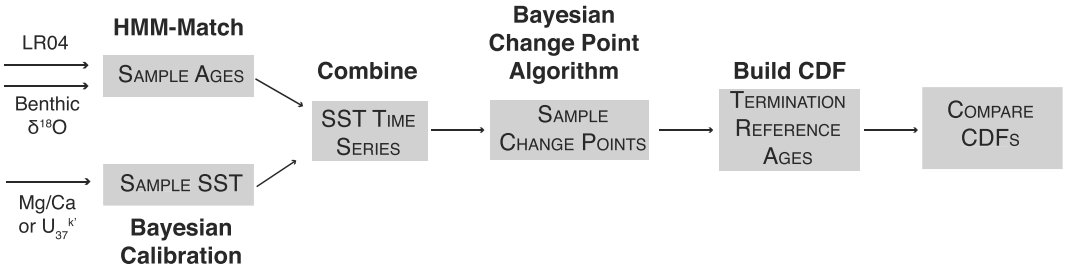


**Figure 1.** Monte Carlo scheme for the estimation of relative termination ages and associated uncertainty.

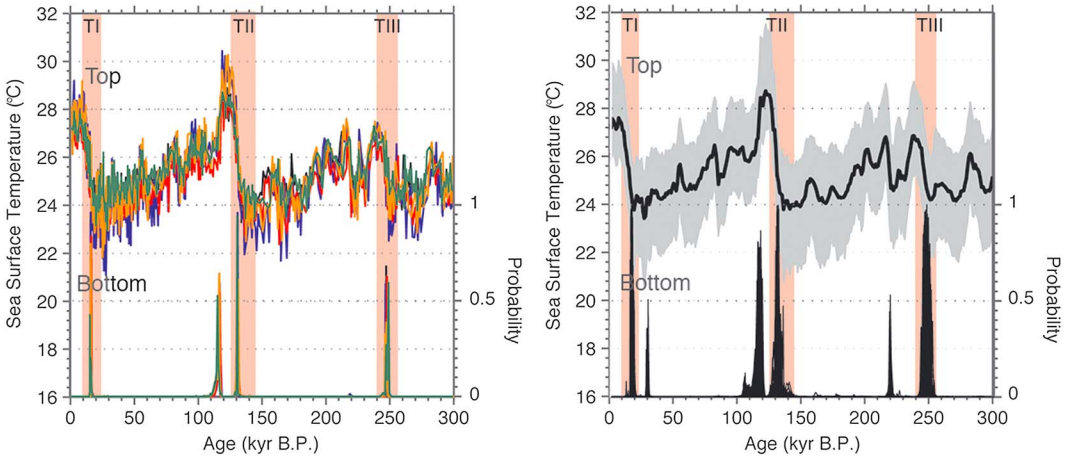


**Figure 2.** (left, top) Five Monte Carlo renditions of the SST time series (illustrated in different colors) for the reference record MD05-2920, whose age model was based on *U. peregrina* (Tachikawa et al., 2014). The Monte Carlo rendition takes into consideration the uncertainty in age from the HMM-Match alignment and the uncertainty in SST, including analytical and calibration errors. (left, bottom) The curves correspond to probability of a change point occurring at each time point for each of the Monte Carlo renditions. Tall, thick spikes indicate relative certainty in the timing of a change point, while shorter and wider peaks indicate more uncertainty (Ruggieri, 2013). (right, top) Median (thick black curve) and 95% confidence interval (shaded area) SST reconstruction for the reference MD05-2920 record inferred from the 1,000 Monte Carlo simulations. (right, bottom) One thousand posterior distributions obtained from the Bayesian change point algorithm. The red vertical bars correspond to the Termination age range considered for the phase calculation.

we assumed that Mg/Ca and $U^{k'}_{37}$ are only affected by SST changes and we, therefore, only considered a one-parameter exponential and linear model, respectively. A more detailed discussion of the methodology can be found in the supporting information (Conte et al., 2006, 1998; Kienast et al., 2012; Prahl et al., 1988; Prahl & Wakeham, 1987; Sadekov et al., 2009; Sonzogni et al., 1997). A discussion about the validity of this assumption is presented in section 3.2.1. Details about the Bayesian calibrations are provided in the supporting information and follow the same mathematical basis described by Khider et al. (2015). The result of this exercise is the generation of 1,000 Monte Carlo SST series, which can then be paired with the 1,000 age models obtained independently as described in section 2.2.1 to create the Monte Carlo realizations of the time series. The Monte Carlo time series were considered independent of each other and therefore contributed equally in the assessment of the terminations timing (Figure 1).

### 2.3. Change Point Detection

We defined the timing of the glacial terminations as the change point in the SST records. A change point identifies when the probability distribution of a time series changes. In this particular instance, we define the termination as a regime shift in SST. To identify the change point in each Monte Carlo realization of the time series, we used the Bayesian Change Point algorithm by Ruggieri (2013) and Ruggieri and Lawrence (2014). This algorithm objectively assesses the uncertainty in both the number and location of change points. Here we used linear models to describe each substring of the Monte Carlo SST time series. We restricted the analysis to the first 300 kyr of record (or the entire length for shorter records) and set the maximum number of change points in any given Monte Carlo record to 10, with a spacing of at least 10 kyr between change points. The Bayesian Change Point algorithm returns the probability of a change point being selected at each time point (Figure 2), drawing 500 samples for each of the 1,000 SST series. Tall, thin spikes indicate relative certainty in the timing of the change point while small, broad pikes indicate a larger uncertainty in the timing of the glacial terminations.

The change point analysis not only returned changes at the deglaciation but also identified other change points in the records. For instance, the transition out of MIS5e (~115 kyr B.P.) in the example record shown in Figure 2 is also identified as a change point. Therefore, we limited the analysis to the spikes that correspond to increases in SST coincident with changes in benthic $\delta^{18}O$ identified in LR04 as transitions from glacial to interglacial (Lisiecki & Raymo, 2005). The targeted intervals for each record are given in Table 2 and illustrated by red bars in Figure 2 and the supporting information. Although the record from ODP1012 spans Termination II, we could not identify the change point corresponding to prior information on the timing of this termination

**Table 2**
*Timing of the Terminations as Observed in the Sea Surface Temperature Records*

| | | Termination I | | Termination II | | Termination III | |
|---|---|---|---|---|---|---|---|
| Name | Proxy | Age range (kyr B.P.) | TI timing (kyr B.P., 95% CI) | Age range (kyr B.P.) | TII timing (kyr B.P., 95% CI) | Age range (kyr B.P.) | TIII timing (kyr B.P., 95% CI) |
| MD05-2920 (ref) | Mg/Ca | 11–22 | 16 (15–18) | 125–145 | 131 (129–133) | 240–255 | 246 (244–249) |
| MD05-2920 | Mg/Ca | 11–24 | 17 (16–20) | 125–145 | 131 (129–134) | 235–255 | 243 (241–246) |
| TR163-19 | Mg/Ca | 10–25 | 17 (14–23) | 125–150 | 132 (130–136) | 235–255 | 249 (244–254) |
| ODP1145 | Mg/Ca | 12–20 | 15 (14–15) | 122–135 | 131 (130–132) | | |
| MD06-3067 | Mg/Ca | 18–23 | 21 (20–23) | 120–140 | 130 (127–133) | | |
| TR163-22 | Mg/Ca | 12–22 | 16 (16–19) | | | | |
| LPAZ-21P | $U^{k'}_{37}$ | 9–35 | 13 (12–21) | 125–165 | 134 (132–142) | | |
| ODP1146 | $U^{k'}_{37}$ | 12–25 | 17 (15–21) | 118–135 | 129 (123–130) | | |
| ODP1143 | $U^{k'}_{37}$ | 10–50 | 22 (18–31) | 125–175 | 134 (132–136) | 235–255 | 242 (239–247) |
| ODP846 | $U^{k'}_{37}$ | 11–40 | 20 (16–33) | 122–150 | 135 (131–138) | | |
| ODP1012 | $U^{k'}_{37}$ | 20–35 | 27 (25–28) | | | 240–255 | 246 (245–247) |
| TR163-19 | $U^{k'}_{37}$ | 10–30 | 13 (12–17) | 130–150 | 133 (130–137) | | |
| MJ0005A-27JC | $U^{k'}_{37}$ | 10–14 | 13 (12–14) | | | | |
| MD97-2151 | $U^{k'}_{37}$ | 11–18 | 13 (12–16) | 130–138 | 136 (133–138) | | |
| MD03-3075 | $U^{k'}_{37}$ | 11–30 | 16 (12–23) | | | | |
| ODP1239 | $U^{k'}_{37}$ | 10–30 | 16 (13–20) | 130–150 | 134 (133–136) | 234–254 | 242 (242–246) |

*Note.* The age range refers to the time interval targeted for analysis, while the timing represents the inferred timing (median 95% confidence interval in parentheses) returned through our Monte Carlo analysis.

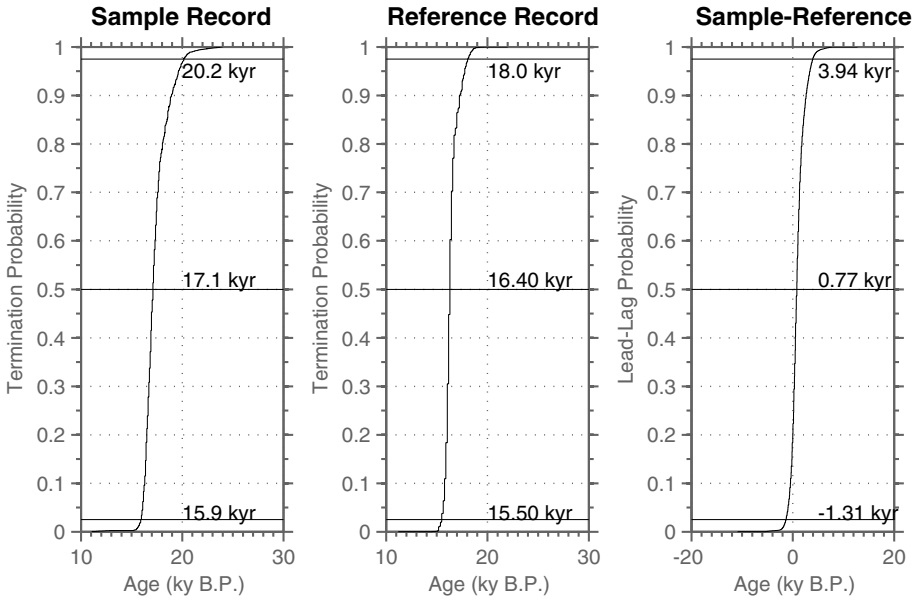


**Figure 3.** (left) Cumulative probability distribution of the absolute Termination I timing in the MD05-2920 record (age model based on *C. wuellerstorfi*). (middle) Cumulative probability distribution of the absolute Termination I timing in the reference MD05-2920 record (age model based on *U. peregrina*). (right) Cumulative probability distribution on the Termination I timing difference between the MD05-2920 record (age model based on *C. wuellerstorfi*) and the reference MD05-2920 record (age model based on *U. peregrina*). The horizontal lines and numbers in each panel indicate the median termination timing and associated 95% confidence interval.

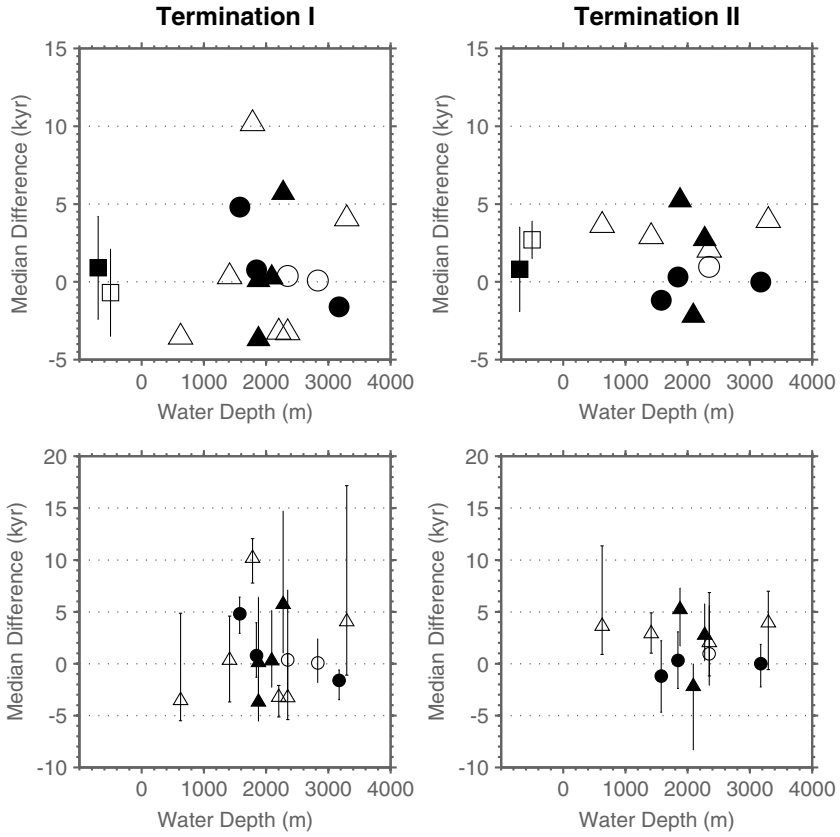


**Figure 4.** (top row) Median relative glacial termination timing as a function of water depth. The relative timing was assessed in reference to the MD05-2920 record (age model based on *U. peregrina*). The filled symbols represent records from the WP, while the empty symbols represent records from the EP. Triangles: SSTs inferred from $U^{k'}_{37}$. Circles: SSTs inferred from Mg/Ca. The squares represent the average timing difference in the WP (filled) and EP (empty) inferred from both Mg/Ca and $U^{k'}_{37}$ records. The error bars represent the standard error on the mean and only includes the uncertainty associated with local environmental factors. (bottom row) Same as top with 95% confidence limits inferred from the Monte Carlo trials. These error bars take into consideration the uncertainty in age, SST, and change point but not the uncertainty associated with local environmental factors.

and we, therefore, omitted this record for Termination II. The change point probability across all Monte Carlo simulations was used to determine the cumulative probability distributions (CDF) of termination ages in each record, including the reference record (Figure 3). The absolute median termination timing and its associated 95% confidence interval were then directly inferred from the CDF (Table 2). Because the absolute age is prone to errors in the LR04 curve, we calculated the difference in absolute ages between a particular record and the reference record (WP core MD05-2920, age model based on the benthic curve obtained from *U. peregrina*) for each of the glacial terminations and propagated the associated uncertainty in this estimate. A positive number (Figure 4) indicates that the termination in a particular record occurred before the termination in the reference record. A full mathematical description of the phase calculation is provided in the supporting information.

## 3. Results and Discussion

The median and 95% confidence intervals on the relative timing of the glacial terminations for the 15 records considered here range from −4.5 kyr to 10.2 kyr (mean: 0 kyr) and from 2.8 kyr to 18.3 kyr (mean: 7.3 kyr), respectively (Figure 4, Table 3, and supporting information). This large uncertainty is not unexpected and reflects the errors in age, SST, and change point detection. In section 3.1, we explore the relative contribution of these sources of uncertainty for the determination of the relative timing of glacial terminations to provide some guidelines on how to improve the precision of the estimates in future studies. We find no significant relationship among the median timing of Termination I and II between the eastern and western tropical Pacific (Figure 4). We do not have a sufficient number of records for Termination III to estimate the significance of the results, which are presented in the supporting information. We performed Mann-Whitney *U* tests to assess

**Table 3**
*Median (and 95% Confidence Interval Width in Kiloyears) Relative Glacial Termination Timing*

| Name | Proxy | Termination I | Termination II | Termination III |
|---|---|---|---|---|
| MD05-2920 | Mg/Ca | 0.77 (5.26) | 0.3 (5.47) | −3.22 (6.71) |
| TR163-19 | Mg/Ca | 0.38 (9.83) | 0.95 (7.68) | 2.43 (9.87) |
| ODP1145 | Mg/Ca | −1.61 (2.85) | −0.01 (4.11) | |
| MD06-3067 | Mg/Ca | 4.8 (3.49) | −1.19 (6.89) | |
| TR163-22 | Mg/Ca | 0.08 (4.22) | | |
| LPAZ-21P | $U^{k'}_{37}$ | −3.55 (10.36) | 3.62 (10.48) | |
| ODP1146 | $U^{k'}_{37}$ | 0.29 (7.42) | −2.19 (8.31) | |
| ODP1143 | $U^{k'}_{37}$ | 5.72 (13.66) | 2.75 (5.46) | −4.5 (9.06) |
| ODP846 | $U^{k'}_{37}$ | 4.06 (18.27) | 3.94 (7.57) | |
| ODP1012 | $U^{k'}_{37}$ | 10.16 (4.29) | | −0.56 (5.66) |
| TR163-19 | $U^{k'}_{37}$ | −3.27 (6.39) | 2.03 (8.05) | |
| MJ0005A-27JC | $U^{k'}_{37}$ | −3.23 (3.04) | | |
| MD97-2151 | $U^{k'}_{37}$ | −3.69 (4.43) | 5.23 (5.58) | |
| MD03-3075 | $U^{k'}_{37}$ | 0.11 (10.50) | | |
| ODP1239 | $U^{k'}_{37}$ | 0.33 (8.27) | 2.9 (3.88) | −4.20 (6.89) |

*Note.* The relative timing was assessed in reference to the MD05-2920 record with the age model based on *U. peregrina*.

the significance of the differences in mean. We could never reject the null hypothesis that two samples come from the same population at the 5% significance level. The more traditional *t* test, which requires the distribution to be Gaussian, returned the same answer. The results of these significance tests are not surprising given the large uncertainty associated with each record. The large disparity in the timing among cores from the same geographical area could also reflect (1) additional controls on the SST proxy records, which would bias one paleothermometer compared to the other, (2) age biases across different water masses (Stern & Lisiecki, 2014), and/or (3) random noise in the climate system such as localized coastal dynamics or differential preservation at the seafloor. In section 3.2, we investigate the contribution of these various factors.

### 3.1. Timing Uncertainty

The average total uncertainty on the phase relationship across all the records considered here is 7.5 kyr at Termination I, 6.7 kyr at Termination II, and 7.4 kyr at Termination III (Figure 4 and supporting information). In this study, we have considered three main sources of uncertainty on the proxy records: the alignment to the LR04 benthic curve (i.e., the age uncertainty), the uncertainty in the SST reconstruction, and the uncertainty in the change point detection. Each of these sources of uncertainty was propagated into the reported 95% confidence interval.

Because most of the uncertainty in SST is associated with calibration and thus dependent from one sample to the next, we hypothesized that the calibration does not introduce a significant uncertainty in the timing error. To test this hypothesis, we repeated our analysis on the proxy records themselves without conversion to SST but allowing for the white noise resulting from analytical uncertainty, which influences the change point detection (Figure 5). We find that conversion to SST does not affect the overall uncertainty and this step can be omitted in the future for computation purposes.

Therefore, the uncertainty reported in this study mainly stems from age model uncertainty and the change point detection, itself dependent on the age model. The age uncertainty resulting from the alignment to the LR04 curve through the HMM-Match algorithm, expressed as the 95% confidence interval, varies from 0.9 kyr to 10 kyr at the glacial terminations. The large range of uncertainty found among the different records is mainly a function of the resolution of the data (supporting information; Lin et al., 2014). In fact, the correlation between the average resolution of a record and the mean age uncertainty is 0.71 ($p$ value $< 0.01$, Table 1).

The impact of age model uncertainty on the determination of the phase relationship is especially apparent in MD05-2920 (Figure 3) since the age models were derived from two distinct benthic curves based on different species routinely used in paleoceanographic studies but the termination timing was assessed

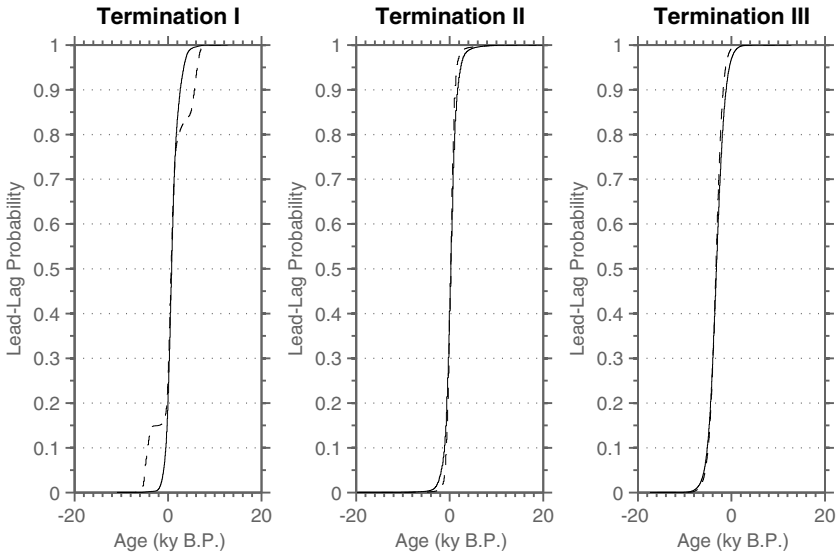


**Figure 5.** Cumulative probability distribution on the (left) Termination I, (middle) Termination II, and (right) Termination III timing difference between the MD05-2920 record (age model based on *C. wuellerstorfi*) and the reference MD05-2920 record (age model based on *U. peregrina*) using the data converted to SST (solid line) and the raw Mg/Ca (dashed line). The calibration does not introduce a large uncertainty in the phase relationship determination, and the conversion to SST can be omitted for computational speed.

on the same SST series. The median phase relationship of SST (95% confidence interval width given in parenthesis) as assessed by independently aligning the $\delta^{18}O$ from two benthic species in the same core is 0.8 kyr (5.3 kyr) at Termination I, 0.3 kyr (5.5 kyr) at Termination II, and −3.2 kyr (6.8 kyr) at Termination III. Since the benthic curves were generated at similar resolution, the age uncertainty is similar for both records and is propagated in the 95% confidence interval on the phase. However, our calculation suggests that the process of aligning a benthic curve to the LR04 curve can create an apparent phasing of up to 3 kyr that is independent of SST proxy or local climate variability and reflects the uncertainty associated with benthic $\delta^{18}O$ (for instance, analytical uncertainty, bioturbation, and/or infaunal versus epifaunal signal). The larger bias and uncertainty at Termination III reflects not only the greater uncertainty in the alignment (supporting information) but also the lower resolution of the data, perhaps associated with stretching of the core at the top (Skinner & McCave, 2003), and the lower signal-to-noise ratio at Termination III.

The average age uncertainty across all records considered in this study at Termination I is lower (2.8 kyr) than at Termination II and Termination III (4.5 kyr and 5.5 kyr, respectively), which mainly indicates the availability of high-resolution records at Termination I. For most of the records presented here, the measurements for the temperature proxies were made at a higher resolution than their benthic $\delta^{18}O$ counterparts, perhaps reflecting the focus of the original studies on SST reconstructions. However, increasing the SST resolution at the expense of the benthic curve used for age modeling may be counterproductive for studies that aim to understand timing differences among various records.

The last source of uncertainty is in the location of the change points corresponding to the glacial terminations, itself dependent on age model uncertainty. In order to evaluate the relative contribution of these two sources of uncertainty on the overall timing, we used Shannon entropy which is a measure of uncertainty in information theory. In information theory, entropy represents the uncertainty associated with a message. If the message is close to random, then its entropy increases. This measure has three advantages: (1) it can be estimated directly for the joint probability distribution of two or more variables or samples drawn from these distributions; (2) it directly accounts for the dependence and thus the correlation between variables; and (3) it is a very well-established measure of uncertainty (Cover & Thomas, 1991; Shannon, 1948). A full mathematical description is given in the supporting information. We find that age uncertainty represents 76% to nearly 100% of the total uncertainty (Figure 6). We find no significant relationship between the absolute age uncertainty and its relative contribution to the total uncertainty ($r = 0.3, p > 0.05$). However, the contribution of age uncertainty to the overall uncertainty at Termination I is lower than at Termination II and III. Termination I is also characterized by an overall lower age uncertainty. We hypothesize that the increased contribution

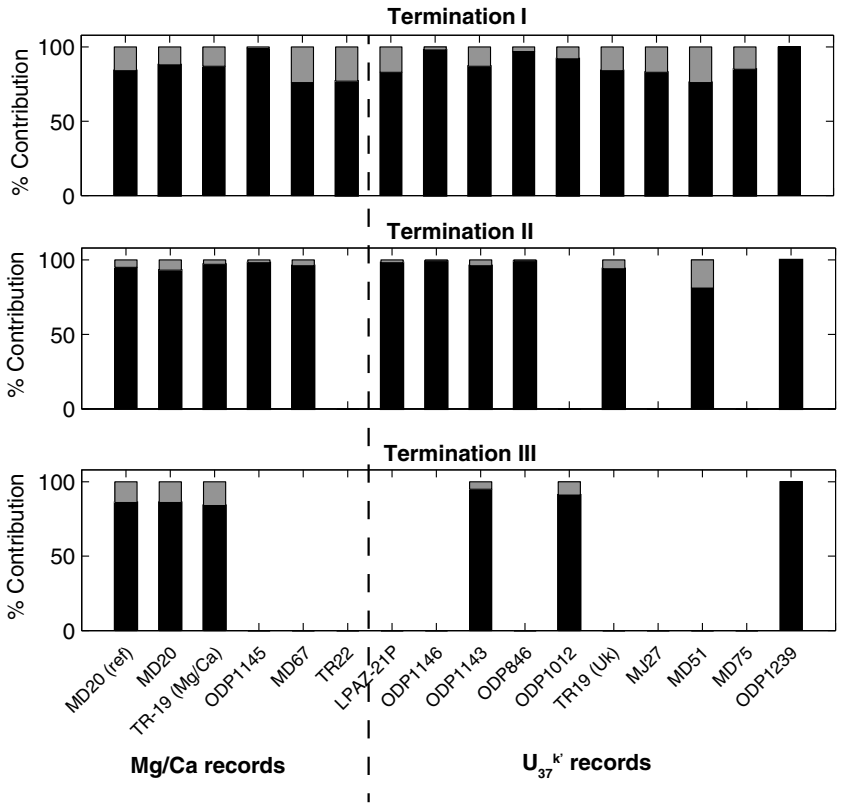


**Figure 6.** Relative contribution of age (black) and change point (grey) uncertainties on the overall error of the (top) Termination I, (middle) Termination II, and (bottom) Termination III timing. The dashed line separates Mg/Ca and $U^{k'}_{37}$ records.

of change point uncertainty at Termination I reflects the relative shortness of the Holocene, which in turns affects the linear models used in the change point algorithm (Ruggieri, 2013). This source of uncertainty is often ignored in paleoclimate studies, but we have demonstrated here that it can have an impact on the interpretation of phase relationships in the climate system.

### 3.2. Biases

#### 3.2.1. Temperature Proxy Biases

Using a compilation of records based on the Mg/Ca and $U^{k'}_{37}$, Timmermann et al. (2014) suggested an earlier deglaciation signal for Termination I in Mg/Ca records compared to $U^{k'}_{37}$ records. This is especially apparent in records from the EP in their original study. They attributed these different termination onsets to seasonal biases among the proxies. Differences between the two proxy reconstructions may be spatially systematic, affecting all the tropical Pacific records similarly. For instance, disparate ecological constraints on the proxy-producing organism (namely, seasonality; e.g., Laepple & Huybers, 2013; Leduc et al., 2010; Lohmann et al., 2013; Schneider et al., 2010; Timmermann et al., 2014) would bias the deglacial response to insolation changes toward a particular season. Similarly, secondary environmental factors such as the effect of salinity on the incorporation of Mg into the foraminiferal calcite lattice (e.g., Hönisch et al., 2013; Khider et al., 2015; Kisakürek et al., 2008; Lea et al., 1999) may create a systematic bias in the timing estimates from Mg/Ca and $U^{k'}_{37}$ arising from global ice volume changes.

However, random processes can also play a large role in the overall uncertainty. Lateral transport through oceanic current (Ohkouchi et al., 2002), postdepositional influences on Mg/Ca (Regenberg et al., 2014), and $U^{k'}_{37}$ (Gong & Hollander, 1999; Hoefs et al., 1998), and the water depth at which the temperature signal is being recorded are examples of random processes that would create disparate conditions in the world ocean, adding random noise to our estimates. For instance, since *G. ruber* is a symbiont-bearing foraminifer and alkenones are produced by photosynthetic coccolithophorids, these proxies should register the temperature

of the photic zone. In oceanic regions where the photic zone extends below the surface mixed layer, the sedimentary signal may not strictly represent SST but rather a composite temperature of the mixed layer and the thermocline (e.g., Müller et al., 1998; Prahl et al., 2006).

We find no statistically significant biases associated with the use of the Mg/Ca or $U^{k'}_{37}$ proxies (Figure 4). The TR163-19 core, in which both proxies have been measured (Table 1), further allows testing for the consistency of termination timing offsets between the two proxies, independent of age model errors. At Termination I, the Mg/Ca-based SST yields a deglacial onset earlier than alkenone-based SST by 3.7 kyr. On the other hand, at Termination II, the alkenone-based SST record leads the deglacial onset in Mg/Ca by 1.0 kyr. The discrepancy between the two terminations results from noise associated with the different proxies, including the effect of local environmental factors on the proxies (e.g., ocean currents), and represents an additional source of uncertainty not accounted for in our model. Therefore, we conclude that the systematic errors affecting the Mg/Ca and alkenone proxies are smaller than the random noise within each proxy in our database ($n = 15$). Identifying and possibly accounting for the biases between the two SST proxies awaits a larger database.

#### 3.2.2. Water Mass Bias

A recent study by Stern and Lisiecki (2014) suggests that the deglacial onset of benthic $\delta^{18}$O changes are not globally synchronous, with ~1 kyr lag in the intermediate Pacific (1000–2000 m water depth) compared to the deep Pacific. However, this estimate is sensitive to the identification method, which was different than the one employed here. In their original study, Stern and Lisiecki (2014) defined the glacial termination onset "as the first stacked $\delta^{18}$O point that is at least 0.1‰ lighter than the maximum $\delta^{18}$O value" rather than using the change point algorithm by Ruggieri (2013). Applying the Bayesian methodology to the regional stacks returns a similar termination timing in the deep and intermediate Pacific (supporting information). A plot of the median termination timings for each record as a function of depth (Figure 4) does not show any significant correlation between timing and water depth ($r = 0.08$, $p$ value = 0.78 for Termination I and $r = -0.09$, $p$ value = 0.78 for Termination II). Because we found a very weak and insignificant correlation between depth and timing in these data, there is no reason to attempt to control for this factor in our analysis.

### 3.3. Timing of SST Changes in the Tropical Pacific

Averaging over all the available records should lead to a more precise estimate of the termination timing difference between the WP and EP. The average difference in the median Termination I timing between records from the WP and the reference MD05-2920 record is 0.9 ± 3.3 kyr, where the uncertainty is expressed as the standard error on the mean. Repeating the calculation for the EP records suggests an average timing difference of −0.7 ± 2.8 kyr with the reference record, resulting in an average phase between the WP and EP of 1.6 ± 4.3 kyr. Since the 95% confidence band widely overlaps 0, there is no evidence in these combined records to support the hypothesis of earlier SST change in the WP than in the EP. Repeating our calculation for Termination II and Termination III yields phase estimates of −1.9 ± 3.0 kyr and −3.1 ± 3.4 kyr, respectively. The finding of confidence limits widely overlapping 0 and in the opposite direction of Termination I shows no support of the hypothesized lead of WP over EP.

Based on the Mann-Whitney $U$ test and $t$ test, we cannot reject the null hypothesis that the data sets are the same at the 5% significance level. Therefore, the change in the relationship between the EP and the WP at Termination I compared to Termination II and Termination III does not hold any climate significance. The large uncertainty in our estimates prevents any conclusions about the phase relationship between the EP and WP at the terminations on millennial timescales. Since the random sources of uncertainty dominate the overall uncertainty, increasing the size of the database, especially with high-resolution records which tend to carry a lower age uncertainty, would lead to better estimates of relative termination timing across the tropical Pacific. This is especially true for Terminations II and III to be able to test whether the tropical Pacific response is consistent across several glacial terminations.

Assuming that there should be a difference in the termination timing between the WP and EP and that our estimate of the uncertainty expressed as the error on the mean is an accurate approximation of the actual variance, then we can calculate the number of samples (i.e., records) needed to achieve an accuracy of 1,000 years using the formula $\sigma_T = \frac{\sigma_S}{\sqrt{n}}$, where $\sigma_T$ represents the total standard deviation, $\sigma_S$ is the sample standard deviation (i.e., ±3.3 kyr), and $n$ is the number of records ($n = 7$ in the WP at Termination I). We find that we would require 77 records of the same resolution as the records comprising the current data set to determine the relative timing of a termination within 1,000 years (305 samples for a precision of 500 years). However, if the tropical Pacific plays an important role during termination, then the assumption that the phase relationship

between the WP and EP is constant across all terminations should be valid. Therefore, the number of individual records needed for such an estimate decreases to $n = 25$ for records spanning three glacial-interglacial cycles and to $n = 20$ for records spanning four cycles. These results clearly indicate the need for improvements in the technology for estimating the ages of stratigraphic records.

### 3.4. Caveats

In this study, we modeled terminations using linear models for each substring. While these represent a reasonable first-order assumption, improved models of glacial-interglacial changes such as a sawtooth model may reduce uncertainty in the change point aspect of our work. Röthlisberger et al. (2008) used RAMPFIT (Mudelsee, 2000) to identify the termination but had to allow for exceptions to model some terminations. For instance, an idealized sawtooth model may not be able to capture the cooling in Marine Isotope Stage (MIS) 7, which is a real feature of the climate system. This may lead to biased estimates at Termination III. Furthermore, this model may be inappropriate for SST records that exhibit a slower warming trend than would otherwise be implied in an abrupt termination model such as the warming for Termination II in cores MD06-3067 (Figure S25), ODP1145 (Figure S33), or TR163-19 (Figure S41). Finally, the sawtooth model would have to account for the lower frequency variability superimposed on the glacial-interglacial cycle (e.g., core TR163-19, Figure S41). Therefore, our simple linear model should be appropriate to estimate the termination timing in SST records from the tropical Pacific. Furthermore, since most of the uncertainty is associated with age, improving upon the change point model would only have a limited effect on the overall precision.

HMM-Match assumes a constant variance in benthic $\delta^{18}$O over the full alignment interval. The use of probabilistic models that provide more specific estimates of variance by garnering information from multiple records should help reduce uncertainty in the assignment of age. Such models are a probabilistic extension of the model used to build the LR04 stack, and we await these developments.

Better constraints on the timing of Termination I should be possible through the use of radiocarbon dating. To examine this, we created an age model for cores where $^{14}$C AMS ages were available using the Bchron Bayesian software (Haslett & Parnell, 2008). This analysis shows age uncertainty comparable to, if not greater than, the uncertainty associated with HMM-Match (supporting information). Furthermore, a recent study (Timmermann et al., 2014) showed that the onset of Termination I in Mg/Ca records from the EP occurred on average ~2 kyr prior to the onset in alkenone records from the same region. This estimate is within the uncertainty of the phase relationship among the two proxies inferred in this study for Termination I. The age models for the sedimentary records referenced in the Timmermann et al. (2014) study were based on radiocarbon dating, suggesting that the two techniques yield similar results.

Exact calculation of probability distributions using a forward-backward algorithm, which are possible with HMM-Match and the Bayesian Change Point algorithm, would eliminate uncertainty stemming from Monte Carlo sampling. However, we expect only a small improvement from this because the large 1,000 samples used in this work will be close to the exact solution obtained by forward-backward values.

## 4. Conclusions

We investigated the relative timing of the last three glacial terminations in the EP and the WP using 15 published records of SST variability inferred from either the *G. ruber* Mg/Ca or $U^{k'}_{37}$ paleothermometers. The novelty of our study is in the quantitative assessment of the various sources of uncertainties inherent to paleoceanographic records and relative timing analysis. Specifically, we used a Monte Carlo process to infer possible realizations of the time series based on age model uncertainty stemming from the alignment to the LR04 curve and SST uncertainty, including that arising from the instrumental analyses and the calibration. Finally, we considered the uncertainty associated with the detection of the glacial terminations, which we took here as the change point in the SST series.

We found that the uncertainty on the relative timing of the glacial termination is large, on the order of several thousand years, and stems mostly (~90%) from age model uncertainty. Therefore, increasing the resolution of the benthic $\delta^{18}$O curve may improve estimates in the future. Our calculations suggest that phase uncertainty estimates of less than 3 kyr correspond to records with an average age uncertainty of 2 kyr and a resolution of less than 0.5 kyr. Finally, we demonstrated that random errors originating from the proxies themselves or from within the climate system are more important than their systematic counterparts (i.e., systematic differences between the Mg/Ca and $U^{k'}_{37}$ thermometers or age uncertainty associated with water mass differences).

Therefore, averaging the median timing across all sites may lead to more accurate and precise estimates of the termination timing in the WP and EP than considering each record separately. However, at this time, we are lacking a sufficient number of records to identify any significant phase relationships within the tropical Pacific across all three glacial terminations. Furthermore, understanding the mechanisms through which the climate system responds to orbital insolation changes will require comparing the phase relationships of proxy records to the insolation curve, therefore requiring the use of absolute chronologies. In turn, these will be prone to higher uncertainties and, therefore, will require more paleoproxy records than available at this time.

**Acknowledgments**
The project is funded by National Science Foundation grants OCE1025444 to Lisiecki and OCE1025438 to Lawrence. Data are available in LiPD format on GitHub (https://github.com/khider/DeglacialTiming) and LinkedEarth (http://wiki.linked.earth/Khider.DeglacialTiming). Codes are available on GitHub (https://github.com/khider/DeglacialTiming).

## References

An, S.-I., Timmermann, A., Bejerano, L., Jin, F.-F., Justino, F., Liu, Z., & Tudhope, A. (2004). Modeling evidence for enhanced El Niño–Southern Oscillation amplitude during the Last Glacial Maximum. *Paleoceanography*, *19*, PA4009. https://doi.org/10.1029/2004PA001020

Billups, K. (2015). Timing is everything during deglaciations. *Nature*, *522*, 163–164.

Blaauw, M., & Christen, J. (2011). Flexible paleoclimate age-depth models using an autoregressive gamma process. *Bayesian Analysis*, *6*(3), 457–474. https://doi.org/10.1214/11-BA618

Bolliet, T., Holbourn, A., Kuhnt, W., Laj, C., Kissel, C., Beaufort, L., … Garbe-Schönberg, D. (2011). Mindanao Dome variability over the last 160 kyr: Episodic glacial cooling of the West Pacific Warm Pool. *Paleoceanography*, *26*, PA1208. https://doi.org/10.1029/2010PA001966

Breitenbach, S. F. M., Rehfeld, K., Goswami, B., Baldini, J. U. L., Ridley, H. E., Kennett, D. J., … Marwan, N. (2012). COnstructing Proxy Records from Age models (COPRA). *Climate of the Past*, *8*(5), 1765–1779. https://doi.org/10.5194/cp-8-1765-2012

Brierley, C., Fedorov, A., Liu, Z., Herbert, T., Lawrence, K., & LaRiviere, J. (2009). Greatly expanded tropical warm pool and weakened Hadley circulation in the early Pliocene. *Science*, *323*, 1714–1718.

Broecker, W., & Clark, E. (2003). Glacial-age deep sea carbonate ion concentrations. *Geochemistry, Geophysics, Geosystems*, *4*(6), 1047. https://doi.org/10.1029/2003GC000506

Cane, M. (1998). A role for the tropical Pacific. *Science*, *282*, 59–61.

Cheng, X., Zhao, Q., Wang, J., Jian, Z., Xia, P., Huang, B., … Wang, P. (2004). *Data report: Stable isotopes from sites 1147 and 1148* (Vol. 184, pp. 1–12). College Station, TX: Ocean Drilling Program.

Clement, A. C., & Cane, M. (1999a). *A role for the Tropical Pacific Coupled Ocean-Atmosphere System on Milankovitch and Millennial Timescales. Part I: A modeling study of tropical variability* (Vol. 112, pp. 363–371). Washington, DC: American Geophysical Union.

Clement, A. C., & Cane, M. (1999b). *A role for the Tropical Pacific Coupled Ocean-Atmosphere System on Milankovitch and Millennial Timescales. Part II: Global impacts* (Vol. 112, pp. 373–383). Washington, DC: American Geophysical Union.

Clement, A. C., & Peterson, L. C. (2008). Mechanisms of abrupt climate change of the last glacial period. *Reviews of Geophysics*, *46*, RG4002. https://doi.org/10.1029/2006RG000204

Comboul, M., Emile-Geay, J., Evans, M., Mirnateghi, N., Cobb, K. M., & Thompson, D. (2014). A probabilistic model of chronological errors in layer-counted climate proxies: Applications to annually banded coral archives. *Climate of the Past*, *10*, 825–841. https://doi.org/10.5194/cp-10-825-2014

Conroy, J., Overpeck, J., & Cole, J. (2010). El Niño/Southern Oscillation and changes in the zonal gradient of tropical Pacific sea surface temperature over the last 1.2 ka. *PAGES News*, *18*(1), 32–34.

Conte, M., Sicre, M.-A., Rühlemann, C., Weber, J., Schulte, S., Schulz-Bull, D., & Blanz, T. (2006). Global temperature calibration of the alkenone unsaturation index ($U^{k'}_{37}$) in surface waters and comparison with surface sediments. *Geochemistry, Geophysics, Geosystems*, *7*, Q02005. https://doi.org/10.1029/2005GC001054

Conte, M., Thompson, A., Lesley, D., & Harris, R. (1998). Genetic and physiological influences on the alkenone/alkenoate versus growth temperature relationship in Emiliania huxleyi and Gephyrocapsa oceanica. *Geochimica et Cosmochimica Acta*, *62*, 51–68.

Cover, T., & Thomas, J. (1991). *Elements of information theory*. Hokoben, NJ: John Wiley.

Denton, G., Anderson, R., Togg weiler, J., Edwards, R. L., Schaefer, J., & Putman, A. (2010). The last glacial termination. *Science*, *328*, 1652–1656. https://doi.org/10.1126/science.1184119

Dubois, N., Kienast, M., Normandeau, C., & Herbert, T. D. (2009). Eastern equatorial Pacific cold tongue during the Last Glacial Maximum as seen from alkenone paleothermometry. *Paleoceanography*, *24*, PA4207. https://doi.org/10.1029/2009PA001781

Fraser, N., Kuhnt, W., Holbourn, A., Bolliet, T., Andersen, N., Blanz, T., & Beaufort, L. (2014). Precipitation variability within the West Pacific Warm Pool over the past 120 ka: Evidence from the Davao Gulf, southern Philippines. *Paleoceanography*, *29*, 1094–1110. https://doi.org/10.1002/2013PA002599

Gong, C., & Hollander, D. (1999). Evidence for differential degradation of alkenones under contrasting bottom water oxygen conditions: Implications for paleotemperature reconstruction. *Geochimica and Cosmochimica Acta*, *63*(3/4), 405–411.

Govin, A., Capron, E., Tzedakis, P. C., Verheyden, S., Ghaleb, B., Hillaire-Marcel, C., … Zahn, R. (2015). Sequence of events from the onset to the demise of the last interglacial: Evaluating strengths and limitations of chronologies used in climatic archives. *Quaternary Science Reviews*, *129*, 1–36. https://doi.org/10.1016/j.quascirev.2015.09.018

Grant, K. M., Rohling, E. J., Bar-Matthews, M., Ayalon, A., Medina-Elizalde, M., Ramsey, C. B., … Roberts, A. P. (2012). Rapid coupling between ice volume and polar temperature over the past 150,000 years. *Nature*, *491*(7426), 744–747. https://doi.org/10.1038/nature11593

Haslett, J., & Parnell, A. (2008). A simple monotone process with application to radiocarbon-dated depth chronologies. *Journal of the Royal Statistical Society C*, *57*, 399–418.

Herbert, T., Schuffert, J., Andreasen, D., Heusser, L., Lyle, M., Mix, A., … Herguera, J. (2001). Collapse of the California current during glacial maxima linked to climate change on land. *Science*, *293*, 71–76.

Herbert, T. D., Peterson, L., Lawrence, K., & Liu, Z. (2010). Tropical ocean temperatures over the past 3.5 Myr. *Science*, *328*(5985), 1530–1534.

Hoefs, M. J. L., Versteegh, G. J. M., Rijpstra, W. I. C., de Leeuw, J. W., & Damsté, J. S. S. (1998). Postdepositional oxic degradation of alkenones: Implications for the measurement of palaeo sea surface temperatures. *Paleoceanography*, *13*(1), 42–49. https://doi.org/10.1029/97PA02893

Hoffman, J. S., Clark, P. U., Parnell, A. C., & He, F. (2017). Regional and global sea-surface temperatures during the last interglaciation. *Science*, *355*(6322), 276–279. https://doi.org/10.1126/science.aai8464

Hönisch, B., Allen, K., Lea, D., Spero, H., Eggins, S., Arbuszewski, J., … Elderfield, H. (2013). The influence of salinity on Mg/Ca in planktonic foraminifers—Evidence from cultured, core-top sediments and complementary $^{18}O$. *Geochimica et Cosmochimica Acta*, *121*, 196–213. https://doi.org/10.1016/j.gca.2013.07.028

Huybers, P., & Wunsch, C. (2004). A depth-derived Pleistocene age model: Uncertainty estimates, sedimentation variability, and nonlinear climate change. *Paleoceanography*, *19*, PA1028. https://doi.org/10.1029/2002PA000857

Khider, D., Huerta, G., Jackson, C., Stott, L., & Emile-Geay, J. (2015). A Bayesian, multivariate calibration for Globigerinoides ruber Mg/Ca. *Geochemistry, Geophysics, Geosystems*, *16*, 2916–2932. https://doi.org/10.1002/2015GC005844

Khider, D., Jackson, C. S., & Stott, L. D. (2014). Assessing millennial-scale variability during the Holocene: A perspective from the western tropical Pacific. *Paleoceanography*, *29*, 143–159. https://doi.org/10.1002/2013PA002534

Kienast, M., MacIntyre, G., Dubois, N., Higginson, S., Normandeau, C., Chazen, C., & Herbert, T. D. (2012). Alkenone unsaturation in surface sediments from the eastern equatorial Pacific: Implications for SST reconstructions. *Paleoceanography*, *27*, PA1210. https://doi.org/10.1029/2011PA002254

Kisakürek, B., Eisenhauer, A., Böhm, F., Garbe-Schönberg, D., & Erez, J. (2008). Controls on shell Mg/Ca and Sr/Ca in cultured planktonic foraminiferan, Globigerinoides ruber (White). *Earth and Planetary Science Letters*, *273*, 260–269. https://doi.org/10.1016/j.epsl.2008.06.026

Kopp, R. E., Simons, F. J., Mitrovica, J. X., Maloof, A. C., & Oppenheimer, M. (2009). Probabilistic assessment of sea level during the last interglacial stage. *Nature*, *462*(7275), 863–867. https://doi.org/10.1038/nature08686

Koutavas, A., & Lynch-Stieglitz, J. (2003). Glacial-interglacial dynamics of the eastern equatorial Pacific cold tongue-Intertropical Convergence Zone system reconstructed from oxygen isotope records. *Paleoceanography*, *18*(4), 1089. https://doi.org/10.1029/2003PA000894

Koutavas, A., Lynch-Stieglitz, J., Marchitto, T. J., & Sachs, J. (2002). El Nino-like pattern in ice age tropical Pacific sea surface temperature. *Science*, *297*, 226–230.

Laepple, T., & Huybers, P. (2013). Reconciling discrepancies between $U^{k'}_{37}$ and Mg/Ca reconstructions of Holocene marine temperature variability. *Earth and Planetary Science Letters*, *375*, 418–429. https://doi.org/10.1016/j.epsl.2013.06.006

Lang, N., & Wolff, E. W. (2011). Interglacial and glacial variability from the last 800 ka in marine, ice and terrestrial archives. *Climate of the Past*, *7*(2), 361–380. https://doi.org/10.5194/cp-7-361-2011

Latif, M., Roeckner, E., Mikolajewicz, U., & Voss, R. (2000). Tropical stabilization of the thermohaline circulation in a greenhouse warming simulation. *Journal of Climate*, *13*, 1809–1813.

Lawrence, K., Liu, Z., & Herbert, T. (2006). Evolution of the eastern tropical Pacific through Plio-Pleistocne glaciation. *Science*, *312*(5770), 79–83. https://doi.org/10.1126/science.1120395

Lea, D., Martin, P., Pak, D., & Spero, H. (2002). Reconstructing a 350 kyr history of sea level using planktonic Mg/Ca and oxygen isotope records from a Cocos Ridge core. *Quaternary Science Reviews*, *21*(1–3), 283–293.

Lea, D., Mashiotta, T., & Spero, H. (1999). Controls on magnesium and strontium uptake in planktonic foraminifera determined by live culturing. *Geochimica et Cosmochimica Acta*, *63*(16), 2369–2379.

Lea, D., Pak, D., Belanger, C., Spero, H., Hall, M., & Shackleton, N. J. (2006). Paleoclimate history of Galapagos surface waters over the last 135,000 years. *Quaternary Science Reviews*, *25*, 1152–1167.

Leduc, G., Schneider, R., Kim, J.-H., & Lohmann, G. (2010). Holocene and Eemian sea surface temperature trends as revealed by alkenone and Mg/Ca paleothermometry. *Quaternary Science Reviews*, *29*, 989–1004. https://doi.org/10.1016/j.quascirev.2010.01.004

Lee, S., & Kim, K. H. (2003). The dynamical relationship between subtropical and eddy-driven jets. *Journal of Atmospheric Sciences*, *60*, 1490–1503.

Li, L., Li, Q., Tian, J., Wang, P., Wang, H., & Liu, Z. (2011). A 4-Ma record of thermal evolution in the tropical western Pacific and its implications on climate change. *Earth and Planetary Science Letters*, *309*(1–2), 10–20. https://doi.org/10.1016/j.epsl.2011.04.016

Lin, L., Khider, D., Lisiecki, L., & Lawrence, C. (2014). Probabilistic sequence alignment of stratigraphic records. *Paleoceanography*, *29*, 976–989. https://doi.org/10.1002/2014PA002713

Lisiecki, L. E, & Lisiecki, P. A. (2002). Application of dynamic programming to the correlation of paleoclimate records. *Paleoceanography*, *17*(4), 1049. https://doi.org/10.1029/2001PA000733

Lisiecki, L., & Raymo, M. (2005). A Pliocene-Pleistocene stack of 57 globally distributed benthic $\delta^{18}$O records. *Paleoceanography*, *20*, PA1003. https://doi.org/1010.1029/2004PA001071

Lohmann, G., Pfeiffer, M., Laepple, T., Leduc, G., & Kim, J. H. (2013). A model-data comparison of the Holocene global sea surface temperature evolution. *Climate of the Past*, *9*(4), 1807–1839. https://doi.org/10.5194/cp-9-1807-2013

Mann, M., Zhang, Z., Rutherford, S., Bradley, R., Hughes, M., Shindell, D., … Ni, F. (2009). Global signatures and dynamical origins of the Little Ice Age and Medieval Climate Anomaly. *Science*, *326*, 1256–1260. https://doi.org/10.1126/science.1177303

Marcott, S. A., Shakun, J. D., Clark, P. U., & Mix, A. C. (2013). A reconstruction of regional and global temperature for the past 11,300 years. *Science*, *339*(6124), 1198–201. https://doi.org/10.1126/science.1228026

Marino, G., Rohling, E. J., Rodriguez-Sanz, L., Grant, K. M., Heslop, D., Roberts, A. P., … Yu, J. (2015). Bipolar seesaw control on last interglacial sea level. *Nature*, *522*(7555), 197–201. https://doi.org/10.1038/nature14499

Martinson, D., Pisias, N., Hays, J., Imbrie, J., Moore, T., & Shackelton, N. (1987). Age dating and the orbital theory of the ice ages: Development of a high-resolution 0 to 300,000-year chronostratigraphy. *Quaternary Research*, *27*, 1–30.

Mudelsee, M. (2000). Ramp function regression: A tool for quantifying climate transitions. *Computers and Geosciences*, *26*, 293–307.

Müller, P., Kirst, G., Ruhland, G., von Storch, I., & Rosell-Melé, A. (1998). Calibration of the alkenone paleotemperature index $u^{k'}_{37}$ based on core-tops from the eastern south Atlantic and the global ocean (60n-60s). *Geochimica et Cosmochimica Acta*, *62*, 1757–1772.

Ohkouchi, N., Eglinton, T. I., Keigwin, L. D., & Hayes, J. M. (2002). Spatial and temporal offsets between proxy records in a sediment drift. *Science*, *298*(5596), 1224–1227. https://doi.org/10.1126/science.1075287

Oppo, D., & Sun, Y. (2007). Amplitude and timing of sea surface temperature change in the northern South China Sea: Dynamic link to the East Asian Monsoon. *Geology*, *33*, 785–788.

Otto-Bliesner, B., Brady, E., Shin, S.-I., Liu, Z., & Shields, C. (2003). Modeling El Niño and its tropical teleconnections during the last glacial-interglacial cycle. *Geophysical Research Letters*, *30*(23), 2198. https://doi.org/10.1029/2003GL018553

Paillard, D. (2015). Quaternary glaciations: From observations to theories. *Quaternary Science Reviews*, *107*, 11–24. https://doi.org/10.1016/j.quascirev.2014.10.002

Parrenin, F., Masson-Delmotte, V., Köhler, P., Raynaud, D., Paillard, D., Schwander, J., … Jouzel, J. (2013). Synchronous change of atmospheric $CO_2$ and Antarctic temperature during the last deglacial warming. *Science*, *339*, 1060–1063.

Pierrehumbert, R. (2000). Climate change and the tropical Pacific: The sleeping dragon wakes. *Proceeding of the National Academy of Sciences*, *94*(4), 1355–1358.

Prahl, F. G., Mix, A. C., & Sparrow, M. A. (2006). Alkenone paleothermometry: Biological lessons from marine sediment records off western South America. *Geochimica et Cosmochimica Acta*, *70*(1), 101–117. https://doi.org/10.1016/j.gca.2005.08.023

Prahl, F., Muehlhausen, L., & Zahnle, D. (1988). Further evaluation of long-chain alkenones as indicators of paleoceanograhic conditions. *Geochimica et Cosmochimica Acta*, *52*, 2303–2310.

Prahl, F. G., & Wakeham, S. (1987). Calibration of unsaturation patterns in long-chain ketone compositions for paleotemperature assessment. *Nature*, *330*, 367–369.

Prell, W., Imbrie, J., Martinson, D., Morley, J., Pisias, N., Shackelton, N., & Streeter, H. (1986). Graphic correlation of oxygen isotope stratigraphy: Application to late Quaternary. *Paleoceanography*, *1*, 137–162. https://doi.org/10.1029/PA001i002p00137

Regenberg, M., Regenberg, A., Garbe-Schonberg, D., & Lea, D. (2014). Global dissolution effects on planktonic foraminiferal Mg/Ca ratios controlled by the calcite-saturation state of bottom waters. *Paleoceanography*, *29*, 127–142. https://doi.org/10.1002/2013PA002492

Rincón-Martínez, D., Lamy, F., Contreras, S., Leduc, G., Bard, E., Saukel, C., … Tiedemann, R. (2010). More humid interglacials in Ecuador during the past 500 kyr linked to latitudinal shifts of the equatorial front and the Intertropical Convergence Zone in the eastern tropical Pacific. *Paleoceanography*, *25*, PA2210. https://doi.org/10.1029/2009PA001868

Rodgers, K. B., Lohmann, G., Lorenz, S., Schneider, R., & Henderson, G. M. (2003). A tropical mechanism for Northern Hemisphere deglaciation. *Geochemistry, Geophysics, Geosystems*, *4*(5), 1046. https://doi.org/10.1029/2003GC000508

Rohling, E. J., Foster, G. L., Grant, K. M., Marino, G., Roberts, A. P., Tamisiea, M. E., & Williams, F. (2014). Sea-level and deep-sea-temperature variability over the past 5.3 million years. *Nature*, *508*(7497), 477–482. https://doi.org/10.1038/nature13230

Röthlisberger, R., Mudelsee, M., Bigler, M., de Angeles, M., Fischer, H., Hansson, M., … Wolff, E. (2008). The Southern Hemisphere at glacial terminations: Insights from the Dome C ice core. *Climate of the Past*, *4*, 345–365.

Ruggieri, E. (2013). A Bayesian approach to detecting change points in climatic records. *International Journal of Climatology*, *33*(2), 520–528. https://doi.org/10.1002/joc.3447

Ruggieri, E., & Lawrence, C. (2014). The Bayesian change point and variable selection algorithm: Application to the $\delta^{18}$O proxy record of the Plio-Pleistocene. *Journal of Computational and Graphical Statistics*, *23*(1), 87–110. https://doi.org/10.1080/10618600.2012.707852

Sadekov, A., Eggins, S., De Dekker, P., Ninnemann, U., Kuhnt, W., & Bassinot, F. (2009). Surface and sub-surface seawater temperature reconstruction using Mg/Ca microanalysis of planktonic foraminifera Globigerinoides ruber, Globigerinoides sacculifer and Pelluniatina obliquiloculata. *Paleoceanography*, *24*, PA3201. https://doi.org/10.1029/2008PA001664

Saikku, R., Stott, L., & Thunell, R. (2009). A bi-polar signal recorded in the western tropical Pacific: Northern and Southern Hemisphere climate records from the Pacific Warm Pool during the last ice age. *Quaternary Science Reviews*, *26*(23–24), 2374–2385.

Sambridge, M. (2016). Reconstructing time series and their uncertainty from observations with universal noise. *Journal of Geophysical Research: Solid Earth*, *121*, 4990–5012. https://doi.org/10.1002/2016JB012901

Schmitt, J., Schneider, R., Elsig, J., Leuenberger, D., Lourantou, A., Chappellaz, J., … Fischer, H. (2012). Carbon isotope constraints on the deglacial $CO_2$ rise from ice cores. *Science*, *336*, 711–714. https://doi.org/10.1126/science.1217161

Schmittner, A., & Clement, A. (2002). Sensitivity of the thermohaline circulation to tropical and high latitude freshwater forcing during the last glacial-interglacial cycle. *Paleoceanography*, *17*(2), 1017. https://doi.org/10.1029/2000PA000591

Schmittner, A., Appenzeller, C., & Stocker, T. (2000). Enhanced Atlantic freshwater export during El Niño. *Geophysical Research Letters*, *27*(8), 1163–1166. https://doi.org/10.1029/1999GL011048

Schneider, B., Leduc, G., & Park, W. (2010). Disentangling seasonal signals in holocene climate trends by satellite-model-proxy integration. *Paleoceanography*, *25*, PA4217. https://doi.org/10.1029/2009PA001893

Seager, R., & Battisti, D. (2007). Challenges to our understanding of the general circulation: Abrupt climate change. In T. Schneider & A. H. Sobel (Eds.), *The global circulation of the atmosphere* (pp. 331–371). Princeton: Princeton University Press.

Shackleton, N. (1967). Oxygen isotope analyses and Pleistocene temperatures re-assessed. *Nature*, *215*, 15–17. https://doi.org/10.1038/215015a0

Shackleton, N., Hall, M., & Vincent, E. (2000). Phase relationships between millennial-scale events 64,000–24,000 years ago. *Paleoceanography*, *15*(6), 565–569.

Shakun, J., Clark, P., He, F., Marcott, S., Mix, A., Liu, Z., … Bard, E. (2012). Global warming preceded by increasing carbon dioxide concentrations during the last deglaciation. *Nature*, *484*, 49–55. https://doi.org/10.1038/nature10915

Shannon, C. (1948). A mathematical theory of communication. *The Bell System Technical Journal*, *27*(3), 379–423.

Skinner, L., & McCave, I. (2003). Analysis and modeling of gravity- and piston coring based on soil mechanics. *Marine Geology*, *199*, 181–204.

Son, S. W., & Lee, S. (2005). The response of westerly jets to thermal driving in a primitive equation model. *Journal of Atmospheric Science*, *62*, 3741–3757.

Sonzogni, C., Bard, E., Rostek, F., Dollfus, D., Rosell-Melé, A., & Elington, G. (1997). Temperature and salinity effects on alkenone ratios measured in surface sediments in the Indian Ocean. *Quaternary Research*, *47*, 344–355.

Stanford, J. D., Hemingway, R., Rohling, E. J., Challenor, P. G., Medina-Elizalde, M., & Lester, A. J. (2011). Sea-level probability for the last deglaciation: A statistical analysis of far-field records. *Global and Planetary Change*, *79*(3–4), 193–203. https://doi.org/10.1016/j.gloplacha.2010.11.002

Stern, J. V., & Lisiecki, L. E. (2014). Termination 1 timing in radiocarbon-dated regional benthic $\delta^{18}$O stacks. *Paleoceanography*, *29*, 1127–1142. https://doi.org/10.1002/2014PA002700

Stott, L., Poulsen, C., Lund, S., & Thunell, R. (2002). Super ENSO and global climate oscillations at millennial time scales. *Science*, *297*(5579), 222–226. https://doi.org/10.1126/science.1071627

Stott, L., Timmermman, A., & Thunell, R. (2007). Southern Hemisphere and deep-sea warming led to deglacial atmospheric $CO_2$ rise and tropical warming. *Science*, *318*, 435–438. https://doi.org/10.1126/science.1143791

Tachikawa, K., Timmermann, A., Vidal, L., Sonzogni, C., & Timm, O. E. (2014). $CO_2$ radiative forcing and Intertropical Convergence Zone influences on western Pacific Warm Pool climate over the past 400 ka. *Quaternary Science Reviews*, *86*, 24–34. https://doi.org/10.1016/j.quascirev.2013.12.018

Thirumalai, K., Quinn, T. M., & Marino, G. (2016). Constraining past seawater $\delta^{18}$O and temperature records developed from foraminiferal geochemistry. *Paleoceanography*, *31*, 1409–1422. https://doi.org/10.1002/2016PA002970

Tierney, J. E., & Tingley, M. P. (2014). A Bayesian, spatially-varying calibration model for the TEX86 proxy. *Geochimica et Cosmochimica Acta*, *127*, 83–106. https://doi.org/10.1016/j.gca.2013.11.026

Timmermann, A., Sachs, J., & Timm, O. (2014). Assessing divergent SST behavior during the last 21 ka derived from alkenones and G. ruber-Mg/Ca in the equatorial Pacific. *Paleoceanography*, *29*, 680–696. https://doi.org/10.1002/2013PA002598

Visser, K., Thunell, R., & Stott, L. (2003). Magnitude and timing of temperature change in the Indo-Pacific Warm Pool during deglaciation. *Nature*, *421*(6919), 152–155. https://doi.org/10.1038/nature01297

Waelbroeck, C., Duplessy, J.-C., Michel, E., Labeyrie, L., Paillard, D., & Duprat, J. (2001). The timing of the last deglaciation in north Atlantic climate records. *Nature*, *412*, 724–727. https://doi.org/10.1038/35089060

Yin, J., & Battisti, D. (2001). The importance of tropical sea surface temperature patterns in simulations of Last Glacial Maximum climate. *Journal of climate*, *14*, 565–581. https://doi.org/10.1175/1520-0442(2001)014<0565:TIOTSS>2.0.CO;2

Zhang, W., Braconnot, P., Guilyardi, E., Merkel, U., & Yu, Y. (2008). ENSO at 6 ka and 21 ka from ocean-atmosphere coupled model simulations. *Ciimate Dynamics*, *30*, 745–762. https://doi.org/10.1007/s00382-007-0320-3

Zhao, M., Huang, C.-Y., Wang, C.-C., & Wei, G. (2006). A millennial-scale $U^{k'}_{37}$ sea-surface temperature record from the South China Sea (8°N) over the last 150 ky: Monsoon and sea-level influence. *Palaeogeography, Palaeoclimatology, Palaeoecology*, *326*(1–2), 39–55.